HHS Public Access

Author manuscript

Cell Calcium. Author manuscript; available in PMC 2016 November 01.

Published in final edited form as:

Cell Calcium. 2015 November ; 58(5): 457–466. doi:10.1016/j.ceca.2015.06.013.

Amphetamine activates calcium channels through dopamine transporter-mediated depolarization

Krasnodara N. Cameron, **Ernesto Solis Jr.**, **Iwona Ruchala**, **Louis J. De Felice**, and **Jose M. Eltit**[#]

Department of Physiology and Biophysics, School of Medicine, Virginia Commonwealth University, Richmond, VA 23298

Abstract

Amphetamine (AMPH) and its more potent enantiomer S(+)AMPH are psychostimulants used therapeutically to treat attention deficit hyperactivity disorder and have significant abuse liability. AMPH is a dopamine transporter (DAT) substrate that inhibits dopamine (DA) uptake and is implicated in DA release. Furthermore, AMPH activates ionic currents through DAT that modify cell excitability presumably by modulating voltage-gated channel activity. Indeed, several studies suggest that monoamine transporter-induced depolarization opens voltage-gated Ca^{2+} channels (Ca_V), which would constitute an additional AMPH mechanism of action. In this study we co-express human DAT (hDAT) with Ca^{2+} channels that have decreasing sensitivity to membrane depolarization ($Ca_V1.3$, $Ca_V1.2$ or $Ca_V2.2$). Although S(+)AMPH is more potent than DA in transport-competition assays and inward-current generation, at saturating concentrations both substrates indirectly activate voltage-gated L-type Ca^{2+} channels ($Ca_V1.3$ and $Ca_V1.2$) but not the N-type Ca^{2+} channel ($Ca_V2.2$). Furthermore, the potency to achieve hDAT-Ca_V electrical coupling is dominated by the substrate affinity on hDAT, with negligible influence of L-type channel voltage sensitivity. In contrast, the maximal *coupling-strength* (defined as Ca^{2+} signal change per unit hDAT current) is influenced by Ca_V voltage sensitivity, which is greater in $Ca_V1.3$- than in $Ca_V1.2$-expressing cells. Moreover, relative to DA, S(+)AMPH showed greater *coupling-strength* at concentrations that induced relatively small hDAT-mediated currents. Therefore S(+)AMPH is not only more potent than DA at inducing hDAT-mediated L-type Ca^{2+} channel currents but is a better depolarizing agent since it produces tighter electrical coupling between hDAT-mediated depolarization and L-type Ca^{2+} channel activation.

Graphical Abstract

[#]Corresponding author: Jose M. Eltit, Department of Physiology and Biophysics, School of Medicine, Virginia Commonwealth University, 1101 E. Marshall St. Rm 3-038H, Richmond, VA 23298, Phone: 1-(804)628-4844, Fax: 1-(804)628-3501, jmeltit@vcu.edu.

The authors declare no conflict of interest.

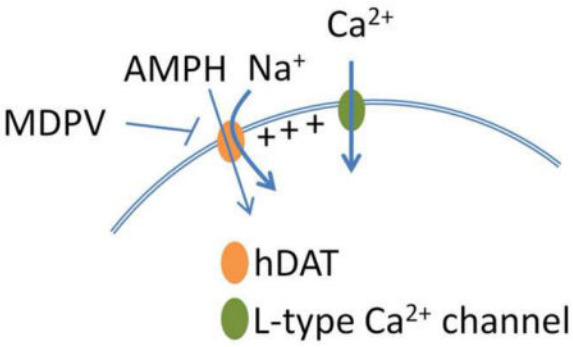

Keywords

Monoamine transporters; neurotransmitter transport; stimulants; serotonin; MDMA; excitability; L-type Ca^{2+} channels

1. Introduction

The dopamine transporter (DAT) is a Na^+/Cl^--dependent symporter expressed in dopaminergic neurons; its principal function is to limit dopamine receptor signaling by restricting the extracellular concentration of dopamine (DA) [1, 2]. Amphetamine (AMPH) is a DAT substrate and its more potent enantiomer, S(+)AMPH, is used therapeutically to treat attention deficit hyperactivity disorder and narcolepsy [2, 3]. AMPH competes with and diminishes DA uptake. In addition, intracellular AMPH disrupts DA's internal stores and induces the reverse transport of DA through DAT, increasing extracellular DA concentration [4, 5]. Accordingly, the activation of dopaminergic pathways in the brain accounts for both the therapeutic properties and addictive liability of AMPH and its active derivatives [2, 6, 7].

An additional level of complexity for AMPH's action in cells is the generation of DAT-mediated, AMPH-induced inward currents [8–11]. Although substrate-induced currents through monoamine transporters are widely accepted [12–15] and they have been implicated in neurotransmitter depletion in the brain [16], the physiological significance of such currents are still under debate [17, 18]. Recently, we showed that depolarization induced by serotonin (5HT) or S(+)3,4-methylenedioxymethamphetamine (MDMA, ecstasy) in skeletal muscle cells engineered to express the human serotonin transporter (hSERT) activates the L-type Ca^{2+} channel $Ca_V1.1$ [19]. Similarly, hSERT-mediated depolarization activates the L-type Ca^{2+} channel $Ca_V1.3$ in HEK cells, whereas hSERT activation is unable to open the N-type Ca^{2+} channel $Ca_V2.2$ under identical experimental conditions [19]. The L-type Ca^{2+} channels are important modulators of signal transduction and excitability in excitable cells. In particular, $Ca_V1.3$ and $Ca_V1.2$ have been extensively studied upstream of Ca^{2+}/calmodulin-dependent protein kinase II (CaMKII) and cAMP response element-binding protein (CREB) signaling pathways in neurons [20–22]. Furthermore, the lower-threshold L-type $Ca_V1.3$ channel is implicated in pace-making in dopaminergic neurons, and in neuroendocrine cells, such as adrenal chromaffin cells [23, 24]. Since L-type channels $Ca_V1.2$ and $Ca_V1.3$ are expressed with monoamine transporters in several excitable cells

[23–29], determining a functional interaction between these two classes of proteins could constitute an additional molecular mechanism of AMPH action.

In the present study we co-expressed the human DAT (hDAT) with $Ca_V1.2$, $Ca_V1.3$ or $Ca_V2.2$ in Flp-In™ T-REx™ 293 cells, and measured the effect of S(+)AMPH- or DA-induced DAT currents on Ca_V activation. These experiments were designed to study the interplay between two variables: 1) the affinity of S(+)AMPH and DA on hDAT, and 2) the voltage sensitivity of the Ca^{2+} channels studied, in achieving effective hDAT-Ca_V coupling. The results show that, regardless of the compound affinity on hDAT, DA and S(+)AMPH can couple indirectly to both L-type channels ($Ca_V1.2$ and $Ca_V1.3$) but not to the N-type channel ($Ca_V2.2$) under identical conditions. In addition, whereas the potency to achieve hDAT-Ca_V electrical coupling is dominated by substrate-hDAT affinity, the *coupling-strength*, defined as the Ca^{2+} signal change per unit hDAT current, is influenced by the sensitivity of Ca^{2+} channels to voltage. Moreover, S(+)AMPH showed larger *coupling-strength* compared to DA at concentrations that induced relatively small hDAT-mediated currents. These results suggest that S(+)AMPH- and DA-induced currents through hDAT are qualitatively different, because the S(+)AMPH-induced current is pharmacologically and electrically stronger at activating L-type channels.

2. Materials and methods

Generation of Flp-In™ T-REx™ cells expressing the human dopamine transporter (Flp-hDAT cells) and Ca_V channel transfection

The generation of the hDAT stable inducible cell line (Flp-hDAT) was done using the Flp-In™ T-REx™ 293 system (Life Technologies). The hDAT cDNA (accession number: NM_001044) was subcloned into the pcDNA5/FRT/TO plasmid and the targeted single site recombination and cell selection were performed as described previously [19]. The Ca^{2+} channels used in this study were $Ca_V2.2$ ($\alpha1_B$, Addgene #26570), $Ca_V1.3$ ($\alpha1_D$, Addgene #26576), $Ca_V1.2$ ($\alpha1_C$ accession number: NM_001136522), β_3 (Addgene #26574) and $\alpha2\delta1$ (Addgene #26575). All these plasmids were kindly provided by Dr. Diane Lipscombe (Department of Neuroscience, Brown University, Providence, Rhode Island, USA) except $Ca_V1.2$, which was kindly provided by Dr. Manfred Grabner (Department of Medical Genetics, Molecular, and Clinical Pharmacology, Innsbruck Medical University, Innsbruck, Austria). The $Ca_V1.2$ cDNA was subcloned into the pcDNA6 expression plasmid thus all $\alpha1$ subunitsare expressed under the same background vector. EGFP expression plasmid was used as a transfection marker. The cells were co-transfected with the DNA ratio $\alpha1{:}\beta3{:}\alpha2\delta1$:EGFP = 1:1:1:0.2 using Fugene 6 (Promega) as the transfection reagent.

Immunofluorescence

Sample fixation and labeling was performed as described earlier [30]. The primary antibody used was a rat monoclonal-anti DAT (Santa Cruz Biotechnology, Cat# sc-32258) and the secondary antibody used was Alexa Fluor 555 goat anti-rat IgG (Invitrogen, Cat# A21434). The nuclei were stained with DAPI. The specimens were visualized in a Zeiss 710 confocal microscope.

[^{3}H]DA Uptake

Flp-DAT cells were counted and 1×10^6 cells were exposed to different concentrations of DA where 1% of the total concentration consisted of [^{3}H]DA. The uptake reaction was performed for 10 min at 37°C in an external solution containing (in mM): 130 NaCl, 4 KCl, 2 $CaCl_2$, 1 $MgCl_2$, 10 HEPES, 10 glucose, pH adjusted to 7.4. Non-specific uptake was determined adding 10 μM methylenedioxypyrovalerone (MDPV, a potent hDAT blocker) [31, 32]. After the incubation period, cells were centrifuged, washed once with PBS, centrifuged again and the cell pellets were resuspended in Ecoscint H (National Diagnostics, Atlanta, GA, USA); radioactivity was measured in a liquid scintillation counter.

Dose response-experiments were fit to the following expression:

$$Y(x) = \frac{Y_{\max}}{1 + 10\exp[\{\log EC_{50} - \log x\} * n]} \quad \text{Eq. 1}$$

Where x is the concentration of the tested compound, Y(x) is the response measured, Y_{max} is the maximal response, EC_{50} is the concentration that yields half-maximal response, and n is the Hill slope parameter. Competition assays were carried out adding a variable concentration of cold DA or cold S(+)AMPH to a constant 10 μM DA solution containing 1% [^{3}H]DA. The inhibition constant (K_i) was estimated using the Cheng-Prusoff equation.

Electrophysiology

Determination of hDAT substrate-induced currents—Patch pipettes made from borosilicate glass capillary tubing and coated with Sylgard were filled with the following internal solution (in mM): 133 K Gluconate, 5.9 NaCl, 1 $CaCl_2$, 0.7 $MgCl_2$, 10 EGTA, 10 HEPES, pH adjusted to 7.2 with KOH. In this condition the pipettes showed a tip resistance of ~4 MΩ. The external solution used was (in mM): 130 NaCl, 4 KCl, 2 $CaCl_2$, 1 $MgCl_2$, 10 HEPES, 10 glucose, pH adjusted to 7.4. Patch-clamp recordings were performed under constant perfusion at 35°C (AutoMate Scientific) and currents were acquired using an Axopatch 200A amplifier, Digidata 1322A acquisition system and Clampex 8.2 software (Molecular Devices); current traces were acquired at 1 kHz at −60 mV holding potential. Drugs were applied at various concentrations following a 30 μM dopamine pre-pulse. Holding currents for all traces were subtracted and divided by the DA pre-pulse peak current for cell to cell comparison.

Determination of Ca^{2+} currents—The Ca^{2+} currents were determined in HEK293T cells transfected with $Ca_V1.2$, $Ca_V1.3$ or $Ca_V2.2$ plus β3, α2δ1, and EGFP as described previously [19]. The external solution used was (in mM): 155 tetraethylammonium (TEA)-Cl, 5 $CaCl_2$, 10 Hepes, pH 7.4 with TEA-OH. The internal solution composition was (in mM): 130 CsCl, 10 Cs-EGTA, 1 $CaCl_2$, 4 MgATP and 10 HEPES, pH adjusted to 7.3 with CsOH. The effective serial resistance was corrected to 80% using the built-in circuit of the Axopatch 200B amplifier (remaining voltage error < 1.2 mV). The leak current was subtracted using a – P/6 protocol. The microelectrodes were made from 8520 glass capillary (Warner Instruments, #64-0817), fire polished, and Sylgard coated. The electrodes tip resistance was ~2.5 MΩ when filled with the internal solution. The whole-cell patch-clamp

parameters of the recordings were: cell capacitance = 22.7 ± 2.3 pF, access resistance = 5.3 ± 0.4 MΩ, and time constant (τ) = 121 ± 16.4 μs (n = 23). The current was set to zero using the "pipette offset" command of the amplifier when the pipette was immersed in the external solution and no additional correction to the liquid-junction potential was performed. The recorded signals were acquired at 10 kHz and filtered at 5 kHz.

The voltage dependence of the I_{Ca} was fit to the following expression:

$$I_{Ca}(V) = \frac{G_{\max}(V - V_r)}{1 + \exp\left(\frac{V_{1/2} - V}{k}\right)} \quad \text{Eq. 2}$$

Where G_{max} is the maximal conductance, V is the test potential, $V_{1/2}$ is the potential at which G = 1/2 G_{max}, k represent a slope parameter, and V_r is the reversal potential.

Determination of intracellular Ca^{2+}

Ca^{2+} determinations were done using the Ca^{2+} sensitive dye Fura-2AM and visualized in an epifluorescence microscope following the procedure and using the equipment described previously [19]. The measurements were done with constant perfusion at 35°C using an external solution with composition (in mM): 130 NaCl, 4 KCl, 2 $CaCl_2$, 1 $MgCl_2$, 10 HEPES, 10 glucose, pH adjusted to 7.4. The Fura-2 signal was acquired switching the excitation wavelength between 340/10 to 380/10 nm using a monochromator as described previously [19], dichroic mirror 490LP and an emission filter 510/40 nm. The acquisition frequency was 3 Hz. All images were background subtracted and the Ca^{2+} signals are shown as $F_{340/380}/F_0$. For dose-response experiments the test values were normalized by the mean of the maximal value of control DA pulses.

Statistics

The data are expressed as mean ± s.e.m. Comparison between two groups of data were made by unpaired two-tailed *t*-test, and when multiple groups were analyzed, one-way ANOVA followed by Tukey's post test was used; $p < 0.05$ was considered significant.

3. Results

Immunostaining in conjunction with confocal microscopy showed membrane localization of hDAT in Flp-hDAT cells three days after doxycycline induction, whereas the parental Flp-In™ T-REx™ 293 (Flp-In) cells showed no hDAT expression (insert, Fig. 1A). In addition, Flp-hDAT cells have specific [^{3}H]DA uptake (EC_{50} = 2.73 ± 0.49 μM, Fig. 1A). Uptake competition assay using cold S(+)AMPH or cold DA yielded inhibition constants (K_i) equal to 0.24 ± 0.03 and 2.06*** ± 0.67 μM respectively (*** = $p < 0.001$ *t*-test n ≥ 9, Fig. 1B).

To determine the extent to which S(+)AMPH- or DA-induced currents in hDAT could activate voltage-gated Ca^{2+} channels, we measured Ca^{2+} signals using the Ca^{2+} sensitive dye Fura-2 in Flp-hDAT cells transfected with $Ca_V1.2$, $Ca_V1.3$, or $Ca_V2.2$. The perfusion of saturating concentrations of DA (10 μM) or S(+)AMPH (5 μM) for 5 s at 35°C induced equivalent Ca^{2+} signals in Flp-hDAT cells expressing $Ca_V1.3$ ($Ca_V1.3$ in Fig. 2). Similar

results were obtained when Flp-hDAT cells expressing $Ca_V1.2$ were exposed to these agents ($Ca_V1.2$ in Fig. 2). The $Ca_V1.3$- and $Ca_V1.2$-mediated signals were blocked by isradipine (2 μM), a potent L-type Ca^{2+} channel blocker ($Ca_V1.3$ and $Ca_V1.2$ in Fig. 2). In contrast, the intracellular Ca^{2+} concentration did not change in Flp-hDAT cells expressing $Ca_V2.2$ when exposed to DA or S(+)AMPH under the same conditions. The sequential exposure to high-K^+ external solution yielded a convincing Ca^{2+} transient demonstrating adequate expression of $Ca_V2.2$ on these cells ($Ca_V2.2$ in Fig. 2). In control assays, in which the α_1 subunit of Ca_V channels is absent in the transfection mix, neither DA, S(+)AMPH nor high-K^+ mobilized Ca^{2+} in Flp-hDAT cells (control in Fig. 2).

To study the voltage sensitivity of Ca^{2+} channels in more detail, $Ca_V1.2$, $Ca_V1.3$, or $Ca_V2.2$ were transiently transfected in HEK293T cells and Ca^{2+} currents were measured under whole-cell voltage-clamp (Fig. 2). In our experimental conditions the test potential that yielded half of the maximal conductance ($V_{1/2}$ in Eq. 2, see experimental procedures section) was −25.6 ± 1.0 mV (n = 8), −3.2 ± 0.8 mV (n = 7) and +5.5 ± 1.0 mV (n = 8) for $Ca_V1.3$, $Ca_V1.2$ and $Ca_V2.2$, respectively (Fig. 2). These results show that although these channels have been categorized as “high-voltage activated” [33], they have notable differences in their response to changes in membrane potential.

To rule out a direct activation of Ca_V channels by DA or S(+)AMPH, intracellular Ca^{2+} was determined in parental Flp-In (no hDAT expression) expressing the L-type Ca^{2+} channels. Neither DA nor S(+)AMPH induce changes in resting Ca^{2+} level in these cells, whereas high K^+-induced Ca^{2+} transients reveal the normal expression of Ca^{2+} channels (Fig. 3A and 3B). MDPV is an abused drug that was found to exert long-lasting inhibitory action of the substrate- induced-DAT conductance and DAT-transport. Indeed, MDPV has higher potency than cocaine blocking both hDAT-mediated currents and DA transport [31, 32, 34]. The perfusion of MDPV (1 μM) abolished S(+)AMPH- or DA-induced Ca^{2+} transients in Flp-hDAT cells expressing either $Ca_V1.2$ or $Ca_V1.3$ (Fig. 3C and 3D); whereas high K^+-induced Ca^{2+} signals were refractory to MDPV treatment. Li^+ ions leak through monoamine transporters in the absence of substrates, and the inward current carried by Li^+ can be as large as the current induced by substrates in Na^+-based external solution [8, 12, 14, 35]. To test whether depolarization mediated by hDAT currents is responsible for Ca_V activation, cells expressing the Ca_V channels were briefly exposed to an external solution in which Na^+ was replaced with equimolar Li^+. As expected, Li^+ induced Ca^{2+} transients in Flp-hDAT cells expressing $Ca_V1.2$ or $Ca_V1.3$ but not in parental Flp-In cells expressing Ca^{2+} channels. In contrast, high-K^+ solution produced Ca^{2+} signals in parental Flp-In and in Flp-hDAT cells expressing these Ca^{2+} channels (Fig. 3E and 3F). Together these results strongly suggest that depolarization is the cause of activation of L-type Ca^{2+} channels in Flp-hDAT cells exposed to hDAT substrates.

Dose-response experiments measuring Ca^{2+} signals in Flp-hDAT cells expressing $Ca_V1.2$ or $Ca_V1.3$ showed that S(+)AMPH has greater potency than DA at activating both L-type Ca^{2+} channels (Fig. 4). In addition, although the difference between DA-elicited EC_{50} values in $Ca_V1.2$- and $Ca_V1.3$-expressing cells showed statistical significance (916 ± 54.3 nM vs 693 ± 25.0 nM, $p < 0.001$ one way-ANOVA, Fig. 4), this small difference is not expected to be biologically relevant. For S(+)AMPH, the EC_{50} values were not significantly different in

cells expressing $Ca_V1.2$ or $Ca_V1.3$ (Fig. 4). These data show that S(+)AMPH is more potent than DA at achieving electrical coupling between hDAT and L-type Ca^{2+} channels. Moreover, channel voltage sensitivity, measured in Fig. 2, only modestly influences the compound potency (EC_{50}) to activate the hDAT- L-type Ca^{2+} channel electrical coupling.

The activation of the L-type Ca^{2+} channels described above requires membrane depolarization. In this study the membrane depolarization is mediated by substrate-induced hDAT currents (I_{hDAT}). To study how I_{hDAT} activates $Ca_V1.2$ and $Ca_V1.3$, the concentration-dependence of I_{hDAT} was measured. S(+)AMPH had greater potency than DA inducing inward currents in Flp-hDAT cells clamped to −60 mV, (Fig. 5); however, S(+)AMPH and DA produced comparable current amplitudes at saturating concentrations (Fig. 5) similar to a previous report [36] (non-normalized currents are shown as supplementary material). To study the relationship between Ca^{2+} signals and hDAT inward currents, the Ca^{2+} signal amplitudes fitted in Fig. 4E were plotted against the fitted hDAT-inward currents of Fig. 5C, which were both evoked by the same compound concentrations (Fig. 5D). Whereas DA generated sigmoidal curves for both $Ca_V1.2$ and $Ca_V1.3$, S(+)AMPH generated a quasi hyperbolic shape for $Ca_V1.3$ and a slightly sigmoidal curve for $Ca_V1.2$ (Fig. 5D). These curves show that S(+)AMPH, compared to DA, generates a relatively larger Ca^{2+} transient in response to smaller hDAT inward currents. To better visualize this difference, the first derivative of the curves shown in Fig. 5D is plotted in Fig. 5E. The value of the slope at every I_{hDAT} defines the "*coupling-strength*" since it quantifies the sensitivity of the system to generate a Ca^{2+} response per unit hDAT inward current. Regardless of the compound tested, $Ca_V1.3$-expressing cells showed higher maximal *coupling-strength* than $Ca_V1.2$-expressing cells (Fig. 5E) suggesting that $Ca_V1.3$, which is more sensitive to voltage than $Ca_V1.2$ (Fig. 2), requires less depolarization mediated by I_{hDAT} to open. Lastly, S(+)AMPH consistently showed higher *coupling-strength* in response to smaller I_{hDAT} magnitudes than DA for both L-type Ca^{2+} channels (Fig. 5E) suggesting that S(+)AMPH- induced currents are more effective than DA-induced currents at depolarizing and activating L-type Ca^{2+} channels.

4. Discussion

Voltage-gated Ca^{2+} channels are composed of the main α_1 subunit and the auxiliary $\alpha_2\delta$, β and γ subunits [37]. The α_1 subunit contributes to the ionic pore and voltage sensor structures, while the others modulate expression, targeting, and function [33, 38, 39]. Neurons and neuroendocrine cells express several $\alpha1$ isoforms. The biophysical properties, location and biochemical partners of the $\alpha1$ subunits regulate Ca^{2+} influx for specific purposes. For example, the opening of L-type Ca^{2+} channels mobilize Ca^{2+}, which in turn activates signaling pathways and gene expression in neurons [21], and Ca^{2+} entry through $Ca_V2.2$ is coupled to neurotransmitter release [40, 41]. The $\alpha1$ isoforms differ in their voltage sensitivity, for instance, Ca_V3 (T-type) channels are activated by slight depolarization (low-voltage activated), whereas Ca_V1 (L-type) and Ca_V2 (N-, P/Q- and R-type) channels activate upon strong depolarization (high-voltage activated) [33]. Despite this categorization, a broad range of voltage sensitivity exists between Ca_V1 and Ca_V2 channels; as shown in Fig. 2, $Ca_V1.3$ is more sensitive to depolarization than $Ca_V1.2$ [42] and $Ca_V2.2$ is the least sensitive channel [43]. For cells expressing monoamine transporters most, if not

all, co-express $Ca_V1.3$ and $Ca_V1.2$, a functional interplay between transporters and channels is plausible. Indeed, DAT-mediated Ca^{2+} channel activation has been described in neurons [44] and AMPH activates Ca^{2+} channels by a NET-dependent mechanism in PC12 cells [45]. Moreover, DAT-mediated currents depolarize neurons [9] and at low concentrations DAT substrates increase electrical excitability of dopaminergic neurons through a mechanism dependent on DAT's substrate-induced current [46, 47]. Interestingly, $Ca_V1.3$ is involved in excitability, accordingly $Ca_V1.3$-knockout mice showed altered pace-making activity in ventral tegmental area dopaminergic neurons [23], leading to the hypothesis that monoamine transporter currents may modulate excitability in neurons through a mechanism that involves L-type Ca^{2+} channels. In addition affecting excitability, as mentioned above, L-type Ca^{2+} channels are also involved in signaling pathway activation. One example of interest is CaMKII, which has been well characterized as an effector of Ca^{2+} currents downstream of L-type Ca^{2+} channels [21, 22]. Interestingly, DAT is a CaMKII substrate and phosphorylated DAT favors the reverse transport of dopamine [48, 49], constituting a possible mechanism by which electrical activity and L-type Ca^{2+} channels may modulate DAT states and dopamine release.

Membrane depolarization induced by monoamine transporters could potentially modulate any voltage-gated channel including not only Ca^{2+}, but also Na^+ and K^+ channels. The functional interaction between transporters and voltage-gated channels described here can depend on several factors such as relative levels of protein expression and clustering of the implicated proteins in membrane microdomains. In addition, biophysical characteristics of the voltage-gated channels, such as voltage sensitivity, and activation/inactivation kinetics, may be decisive factors in the effective electrical coupling with transporters. For instance, tetrodotoxin-sensitive voltage-gated Na^+ channels were not involved in the membrane depolarization induced by serotonin or MDMA in myotubes expressing hSERT since the small but sustained hSERT-mediated depolarization may inactivate the fast Na^+ channels [19]. In another example, the high-voltage-activated Ca^{2+} channel $Ca_V2.2$ is not activated by substrate-induced depolarization through hSERT or hDAT in our heterologous expression system ([19] and Fig. 2), probably because greater depolarization is required for its activation. Case-specific studies would be required to characterize the modulation of specific voltage-gated channels by transporters in native systems.

In the present manuscript we explore how hDAT substrates could modulate Ca^{2+} channel activity in cells; in particular, DAT-mediated substrate-induced membrane depolarization could reach the level of Ca_V channel activation. We tested the functional interaction between hDAT and a single Ca_V channels using heterologous expression, which would be difficult to achieve in native systems. Experiments in Fig. 2 and Fig. 3 show that DA- and AMPH- can induce Ca^{2+} signals in cells expressing L-type Ca_V channels, but these signals required the simultaneous expression of functional hDAT protein. Thus, neither DA nor AMPH can activate L-type Ca^{2+} channels directly (Fig. 3A). Accordingly, both DA and AMPH induced reproducible inward (depolarizing) currents in Flp-hDAT cells (Fig. 5A and 5B), suggesting that depolarization is the cause of L-type Ca_V channel opening upon hDAT activation.

It is well known that hDAT has constitutive conductance to Li^+ in the absence of substrate [8, 12, 14, 35]. Since the intracellular concentration of this ion is zero, the Nernst equilibrium potential for Li^+ during high-Li^+ perfusion is extremely positive. Thus, the cell membrane would depolarize in cells expressing hDAT when exposed to Li^+. As shown in Fig 3C, Flp-hDAT cells must undergo strong depolarization when exposed to Li^+, as is evidenced by activation of Ca_V channels. These data clearly show that hDAT inward current can activate Ca_V channels even in the absence of DA or AMPH, reinforcing the idea that Ca_V channel activation is a consequence of the membrane depolarization and not a direct action of DA or AMPH at Ca_V channels.

Similarly to hSERT [19], hDAT substrate-induced currents are coupled to $Ca_V1.3$ channel activation. Unexpectedly, $Ca_V1.2$ despite its ~20 mV right shift in voltage dependence compared to Cav1.3 (Fig. 2) showed robust electrical coupling with hDAT (Fig. 2). On the other hand, $Ca_V2.2$, which has a ~30 mV right shift in the voltage dependence compared to $Ca_V1.3$, showed no Ca^{2+} channel activation (Fig. 2). These results strongly suggest that L-type but not N-type Ca^{2+} channels are within the activation range of hDAT-mediated depolarization under our experimental conditions. Interestingly, the significant difference in voltage sensitivity between $Ca_V1.2$ and $Ca_V1.3$ plays a little role in the potency (EC_{50}) by which S(+)AMPH or DA activates the channels via hDAT mediated depolarization (Fig. 4). These results suggest that the hDAT mediated depolarization only activates Ca^{2+} channels when the activation threshold falls within the range of depolarization induced by I_{hDAT}. In addition the potency at which a hDAT substrate activate the overall coupling process is dominated by the affinity of the substrate at hDAT.

To quantify the strength required for DA- or S(+)AMPH-induced currents to depolarize the cell membrane and activate Ca^{2+} channels, we introduced the *coupling-strength* index, which measures the Ca^{2+} signal induced per unit I_{hDAT}. Cells expressing $Ca_V1.3$ consistently showed higher *coupling-strength* than $Ca_V1.2$-expressing cells for both hDAT substrates tested. These observations are consistent with the higher voltage sensitivity of $Ca_V1.3$ over $Ca_V1.2$. At lower I_{hDAT} the activated Ca^{2+} conductance may favor further depolarization, thus potentiating the *coupling-strength*, whereas at higher I_{hDAT} amplitudes internal Ca^{2+} may induce channel inactivation decreasing the *coupling-strength*. In any case, the *coupling-strength* would decrease at higher substrate concentration because the system would reach saturation. The *coupling-strength vs.* I_{hDAT} curve (Fig. 5E) is left-shifted for S(+)AMPH compared to DA indicating that S(+)AMPH-induced currents are better at activating Ca^{2+} channels than DA at lower hDAT current amplitudes, further supporting the idea that the S(+)AMPH-induced current is qualitatively different than the DA-induced current. These hDAT currents may differ in kinetics and ionic composition, which in turn could affect the *coupling-strength*; e.g., faster currents would recruit Ca^{2+} channels more quickly leading to greater *coupling-strength*. Time-resolved kinetics that use piezoelectric rapid solution exchange showed that AMPH produces an instantaneous peak current up to several times larger than the steady-state current. The DA-induced current has similar kinetics profile, however, its peak current amplitude is significantly smaller than the one seen for AMPH [50]. The amplitude of the instantaneous current may play a role in the *coupling-strength* of hDAT substrates. The ionic composition of the currents induced by

hDAT substrates is not fully resolved: substrate-induced currents appear to involve both Na^+ and Cl^- conductance. In the context of the HEK cell environment, the presumably low intracellular Cl^- concentration and the resting membrane potential of ~−50 mV [51] renders depolarization due to increased Cl^- conductance unlikely. We and others have recorded substrate-induced inward currents at −60 mV in low-chloride internal solution ([52] and Fig. 5). Under these ionic conditions, the Cl^- current would be outward, and thus, Na^+ must be the charge carrier. In some neurons, higher internal Cl^- concentration, high input resistance and lower resting membrane potential would account for depolarization induced by elevation in Cl^- permeability [53]. Indeed, Cl^- conductance through DAT is implicated in depolarization of midbrain rat dopaminergic neurons and in Caenorhabditis elegans dopaminergic neurons [9, 46]. It is not clear whether different substrates can induce currents with different ionic composition through hDAT but, in any case, conditions in which an inward current is increased would lead to higher *coupling-strength* due to stronger depolarization.

In summary, our results suggest that pharmacologically, S(+)AMPH is more potent than DA at activating hDAT-mediated depolarizing currents, leading to L-type Ca^{2+} channel activation, and the S(+)AMPH-induced current is more tightly coupled than DA to open L-type Ca^{2+} channels.

Supplementary Material

Refer to Web version on PubMed Central for supplementary material.

Acknowledgments

The authors would like to thank Dr. Richard A. Glennon (Department of Medicinal Chemistry, School of Pharmacy, Virginia Commonwealth University, Richmond, VA) for insightful discussions and for providing methylenedioxypyrovalerone used in this work. This study was supported by the National Institute of Health R01 DA033930 (L.J.D.).

References

1. Giros B, Jaber M, Jones SR, Wightman RM, Caron MG. Hyperlocomotion and indifference to cocaine and amphetamine in mice lacking the dopamine transporter. Nature. 1996; 379:606–12. [PubMed: 8628395]
2. Seeman P, Madras BK. Anti-hyperactivity medication: methylphenidate and amphetamine. Mol Psychiatry. 1998; 3:386–96. [PubMed: 9774771]
3. Mignot E. Perspectives in narcolepsy research and therapy. Curr Opin Pulm Med. 1996; 2:482–7. [PubMed: 9363189]
4. Sulzer D, Sonders MS, Poulsen NW, Galli A. Mechanisms of neurotransmitter release by amphetamines: a review. Prog Neurobiol. 2005; 75:406–33. [PubMed: 15955613]
5. Fleckenstein AE, Volz TJ, Riddle EL, Gibb JW, Hanson GR. New insights into the mechanism of action of amphetamines. Annu Rev Pharmacol Toxicol. 2007; 47:681–98. [PubMed: 17209801]
6. Volkow ND, Fowler JS, Wang GJ, Swanson JM. Dopamine in drug abuse and addiction: results from imaging studies and treatment implications. Mol Psychiatry. 2004; 9:557–69. [PubMed: 15098002]
7. Volkow ND, Fowler JS, Wang GJ, Swanson JM, Telang F. Dopamine in drug abuse and addiction: results of imaging studies and treatment implications. Arch Neurol. 2007; 64:1575–9. [PubMed: 17998440]

8. Sonders MS, Zhu SJ, Zahniser NR, Kavanaugh MP, Amara SG. Multiple ionic conductances of the human dopamine transporter: the actions of dopamine and psychostimulants. J Neurosci. 1997; 17:960–74. [PubMed: 8994051]
9. Carvelli L, McDonald PW, Blakely RD, Defelice LJ. Dopamine transporters depolarize neurons by a channel mechanism. Proc Natl Acad Sci U S A. 2004; 101:16046–51. [PubMed: 15520385]
10. DeFelice LJ, Goswami T. Transporters as channels. Annu Rev Physiol. 2007; 69:87–112. [PubMed: 17059369]
11. Rodriguez-Menchaca AA, Solis E Jr, Cameron K, De Felice LJ. S(+)amphetamine induces a persistent leak in the human dopamine transporter: molecular stent hypothesis. British journal of pharmacology. 2012; 165:2749–57. [PubMed: 22014068]
12. Mager S, Min C, Henry DJ, Chavkin C, Hoffman BJ, Davidson N, Lester HA. Conducting states of a mammalian serotonin transporter. Neuron. 1994; 12:845–59. [PubMed: 8161456]
13. Galli A, Blakely RD, DeFelice LJ. Norepinephrine transporters have channel modes of conduction. Proc Natl Acad Sci U S A. 1996; 93:8671–6. [PubMed: 8710929]
14. Lin F, Lester HA, Mager S. Single-channel currents produced by the serotonin transporter and analysis of a mutation affecting ion permeation. Biophys J. 1996; 71:3126–35. [PubMed: 8968583]
15. Sonders MS, Amara SG. Channels in transporters. Curr Opin Neurobiol. 1996; 6:294–302. [PubMed: 8794089]
16. Baumann MH, Bulling S, Benaderet TS, Saha K, Ayestas MA, Partilla JS, Ali SF, Stockner T, Rothman RB, Sandtner W, Sitte HH. Evidence for a role of transporter-mediated currents in the depletion of brain serotonin induced by serotonin transporter substrates. Neuropsychopharmacology. 2014; 39:1355–65. [PubMed: 24287719]
17. Quick MW. Regulating the conducting states of a mammalian serotonin transporter. Neuron. 2003; 40:537–49. [PubMed: 14642278]
18. Sulzer D, Galli A. Dopamine transport currents are promoted from curiosity to physiology. Trends Neurosci. 2003; 26:173–6. [PubMed: 12689764]
19. Ruchala I, Cabra V, Solis E Jr, Glennon RA, De Felice LJ, Eltit JM. Electrical coupling between the human serotonin transporter and voltage-gated Ca(2+) channels. Cell calcium. 2014; 56:25–33. [PubMed: 24854234]
20. Zhang H, Fu Y, Altier C, Platzer J, Surmeier DJ, Bezprozvanny I. Ca1.2 and CaV1.3 neuronal L-type calcium channels: differential targeting and signaling to pCREB. Eur J Neurosci. 2006; 23:2297–310. [PubMed: 16706838]
21. Wheeler DG, Barrett CF, Groth RD, Safa P, Tsien RW. CaMKII locally encodes L-type channel activity to signal to nuclear CREB in excitation-transcription coupling. J Cell Biol. 2008; 183:849–63. [PubMed: 19047462]
22. Wheeler DG, Groth RD, Ma H, Barrett CF, Owen SF, Safa P, Tsien RW. Ca(V)1 and Ca(V)2 channels engage distinct modes of Ca(2+) signaling to control CREB-dependent gene expression. Cell. 2012; 149:1112–24. [PubMed: 22632974]
23. Liu Y, Harding M, Pittman A, Dore J, Striessnig J, Rajadhyaksha A, Chen X. Cav1.2 and Cav1.3 L-type calcium channels regulate dopaminergic firing activity in the mouse ventral tegmental area. J Neurophysiol. 2014; 112:1119–30. [PubMed: 24848473]
24. Marcantoni A, Vandael DH, Mahapatra S, Carabelli V, Sinnegger-Brauns MJ, Striessnig J, Carbone E. Loss of Cav1.3 channels reveals the critical role of L-type and BK channel coupling in pacemaking mouse adrenal chromaffin cells. J Neurosci. 2010; 30:491–504. [PubMed: 20071512]
25. Durante P, Cardenas CG, Whittaker JA, Kitai ST, Scroggs RS. Low-threshold L-type calcium channels in rat dopamine neurons. J Neurophysiol. 2004; 91:1450–4. [PubMed: 14645383]
26. Phillips JK, Dubey R, Sesiashvilvi E, Takeda M, Christie DL, Lipski J. Differential expression of the noradrenaline transporter in adrenergic chromaffin cells, ganglion cells and nerve fibres of the rat adrenal medulla. J Chem Neuroanat. 2001; 21:95–104. [PubMed: 11173223]
27. Sukiasyan N, Hultborn H, Zhang M. Distribution of calcium channel Ca(V)1.3 immunoreactivity in the rat spinal cord and brain stem. Neuroscience. 2009; 159:217–35. [PubMed: 19136044]

28. Takada M, Kang Y, Imanishi M. Immunohistochemical localization of voltage-gated calcium channels in substantia nigra dopamine neurons. Eur J Neurosci. 2001; 13:757–62. [PubMed: 11207810]
29. Schroeter S, Levey AI, Blakely RD. Polarized expression of the antidepressant-sensitive serotonin transporter in epinephrine-synthesizing chromaffin cells of the rat adrenal gland. Mol Cell Neurosci. 1997; 9:170–84. [PubMed: 9245500]
30. Eltit JM, Li H, Ward CW, Molinski T, Pessah IN, Allen PD, Lopez JR. Orthograde dihydropyridine receptor signal regulates ryanodine receptor passive leak. Proc Natl Acad Sci U S A. 2011; 108:7046–51. [PubMed: 21482776]
31. Cameron KN, Kolanos R, Solis E Jr, Glennon RA, De Felice LJ. Bath salts components mephedrone and methylenedioxypyrovalerone (MDPV) act synergistically at the human dopamine transporter. British journal of pharmacology. 2013; 168:1750–7. [PubMed: 23170765]
32. Kolanos R, Solis E Jr, Sakloth F, De Felice LJ, Glennon RA. “Deconstruction” of the abused synthetic cathinone methylenedioxypyrovalerone (MDPV) and an examination of effects at the human dopamine transporter. ACS chemical neuroscience. 2013; 4:1524–9. [PubMed: 24116392]
33. Ertel EA, Campbell KP, Harpold MM, Hofmann F, Mori Y, Perez-Reyes E, Schwartz A, Snutch TP, Tanabe T, Birnbaumer L, Tsien RW, Catterall WA. Nomenclature of voltage-gated calcium channels. Neuron. 2000; 25:533–5. [PubMed: 10774722]
34. Baumann MH, Partilla JS, Lehner KR, Thorndike EB, Hoffman AF, Holy M, Rothman RB, Goldberg SR, Lupica CR, Sitte HH, Brandt SD, Tella SR, Cozzi NV, Schindler CW. Powerful cocaine-like actions of 3,4-methylenedioxypyrovalerone (MDPV), a principal constituent of psychoactive ‘bath salts’ products. Neuropsychopharmacology. 2013; 38:552–62. [PubMed: 23072836]
35. Borre L, Andreassen TF, Shi L, Weinstein H, Gether U. The second sodium site in the dopamine transporter controls cation permeation and is regulated by chloride. J Biol Chem. 2014; 289:25764–73. [PubMed: 25063810]
36. Sitte HH, Huck S, Reither H, Boehm S, Singer EA, Pifl C. Carrier-mediated release, transport rates, and charge transfer induced by amphetamine, tyramine, and dopamine in mammalian cells transfected with the human dopamine transporter. J Neurochem. 1998; 71:1289–97. [PubMed: 9721755]
37. Szpyt J, Lorenzon N, Perez CF, Norris E, Allen PD, Beam KG, Samso M. Three-dimensional localization of the alpha and beta subunits and of the II-III loop in the skeletal muscle L-type Ca2+ channel. J Biol Chem. 2012; 287:43853–61. [PubMed: 23118233]
38. Catterall WA, Perez-Reyes E, Snutch TP, Striessnig J. International Union of Pharmacology. XLVIII. Nomenclature and structure-function relationships of voltage-gated calcium channels. Pharmacol Rev. 2005; 57:411–25. [PubMed: 16382099]
39. Simms BA, Zamponi GW. Neuronal voltage-gated calcium channels: structure, function, and dysfunction. Neuron. 2014; 82:24–45. [PubMed: 24698266]
40. Currie KP. Inhibition of Ca2+ channels and adrenal catecholamine release by G protein coupled receptors. Cell Mol Neurobiol. 2010; 30:1201–8. [PubMed: 21061161]
41. Mochida S, Yokoyama CT, Kim DK, Itoh K, Catterall WA. Evidence for a voltage-dependent enhancement of neurotransmitter release mediated via the synaptic protein interaction site of N-type Ca2+ channels. Proc Natl Acad Sci U S A. 1998; 95:14523–8. [PubMed: 9826733]
42. Lipscombe D, Helton TD, Xu W. L-type calcium channels: the low down. J Neurophysiol. 2004; 92:2633–41. [PubMed: 15486420]
43. Helton TD, Xu W, Lipscombe D. Neuronal L-type calcium channels open quickly and are inhibited slowly. J Neurosci. 2005; 25:10247–51. [PubMed: 16267232]
44. Vaarmann A, Gandhi S, Gourine AV, Abramov AY. Novel pathway for an old neurotransmitter: dopamine-induced neuronal calcium signalling via receptor-independent mechanisms. Cell Calcium. 2010; 48:176–82. [PubMed: 20846720]
45. Kantor L, Zhang M, Guptaroy B, Park YH, Gnegy ME. Repeated amphetamine couples norepinephrine transporter and calcium channel activities in PC12 cells. J Pharmacol Exp Ther. 2004; 311:1044–51. [PubMed: 15340003]

46. Ingram SL, Prasad BM, Amara SG. Dopamine transporter-mediated conductances increase excitability of midbrain dopamine neurons. Nat Neurosci. 2002; 5:971–8. [PubMed: 12352983]

47. Branch SY, Beckstead MJ. Methamphetamine produces bidirectional, concentration-dependent effects on dopamine neuron excitability and dopamine-mediated synaptic currents. J Neurophysiol. 2012; 108:802–9. [PubMed: 22592307]

48. Fog JU, Khoshbouei H, Holy M, Owens WA, Vaegter CB, Sen N, Nikandrova Y, Bowton E, McMahon DG, Colbran RJ, Daws LC, Sitte HH, Javitch JA, Galli A, Gether U. Calmodulin kinase II interacts with the dopamine transporter C terminus to regulate amphetamine-induced reverse transport. Neuron. 2006; 51:417–29. [PubMed: 16908408]

49. Steinkellner T, Yang JW, Montgomery TR, Chen WQ, Winkler MT, Sucic S, Lubec G, Freissmuth M, Elgersma Y, Sitte HH, Kudlacek O. Ca(2+)/calmodulin-dependent protein kinase IIalpha (alphaCaMKII) controls the activity of the dopamine transporter: implications for Angelman syndrome. J Biol Chem. 2012; 287:29627–35. [PubMed: 22778257]

50. Erreger K, Grewer C, Javitch JA, Galli A. Currents in response to rapid concentration jumps of amphetamine uncover novel aspects of human dopamine transporter function. J Neurosci. 2008; 28:976–89. [PubMed: 18216205]

51. Goodwin JS, Larson GA, Swant J, Sen N, Javitch JA, Zahniser NR, De Felice LJ, Khoshbouei H. Amphetamine and methamphetamine differentially affect dopamine transporters in vitro and in vivo. J Biol Chem. 2009; 284:2978–89. [PubMed: 19047053]

52. Schicker K, Uzelac Z, Gesmonde J, Bulling S, Stockner T, Freissmuth M, Boehm S, Rudnick G, Sitte HH, Sandtner W. Unifying concept of serotonin transporter-associated currents. J Biol Chem. 2012; 287:438–45. [PubMed: 22072712]

53. Ben-Ari Y. Excitatory actions of gaba during development: the nature of the nurture. Nat Rev Neurosci. 2002; 3:728–39. [PubMed: 12209121]

Highlights

- Amphetamine (AMPH) and dopamine (DA) induce depolarizing currents through the DA transporter (DAT).
- DAT substrate-induced depolarization activates L-type but not N-type Ca^{2+} channels (Ca_V).
- AMPH is more potent than DA when activating L-type Ca_V.
- The activation of L-type Ca_V displays higher *coupling-strength* with AMPH- than DA-induced currents.
- AMPH action likely involves L-type Ca_V activation.

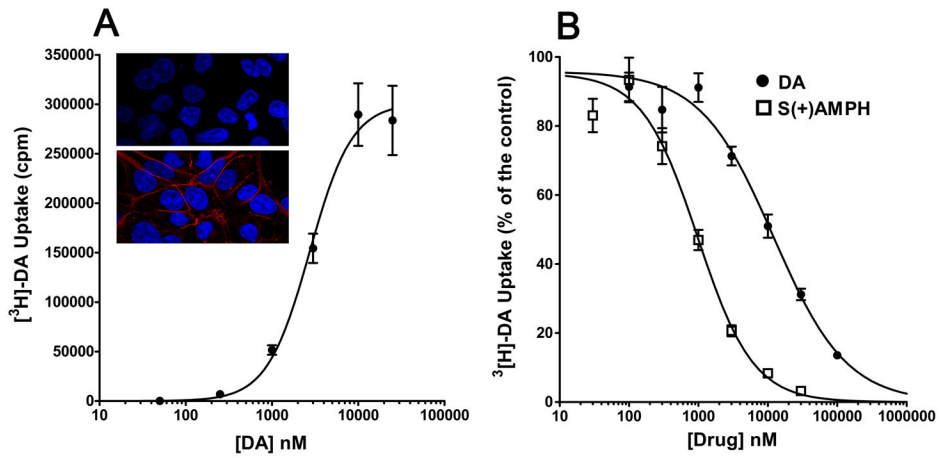

Figure 1. S(+)AMPH is more potent than DA as an hDAT substrate

A. Confocal images show hDAT expression in Flp-hDAT cells (red stain in bottom panel) but not in parental Flp-In^{Tm} T-REx^{TM} cells (top panel). DAPI nuclear staining is depicted in blue. Flp-hDAT cells show specific [^{3}H] DA uptake with the following fitting parameters (see Eq. 1): EC_{50} = 2.73 ± 0.49 μM, Hill slope = 1.8 ± 0.5 (n = 18). B. Competition of [^{3}H]DA uptake using cold dopamine or S(+)AMPH yielded the following fitting parameters (Eq. 1): IC_{50} = 12.05 ± 1.79 μM, Hill Slope = 0.8 ± 0.1 (n = 9) and IC_{50} = 0.98*** ± 0.12 μM, Hill slope = 1.1 ± 0.1 (n = 11, ***p < 0.001 vs. IC_{50} DA competition, *t*-test) for DA and S(+)AMPH, respectively.

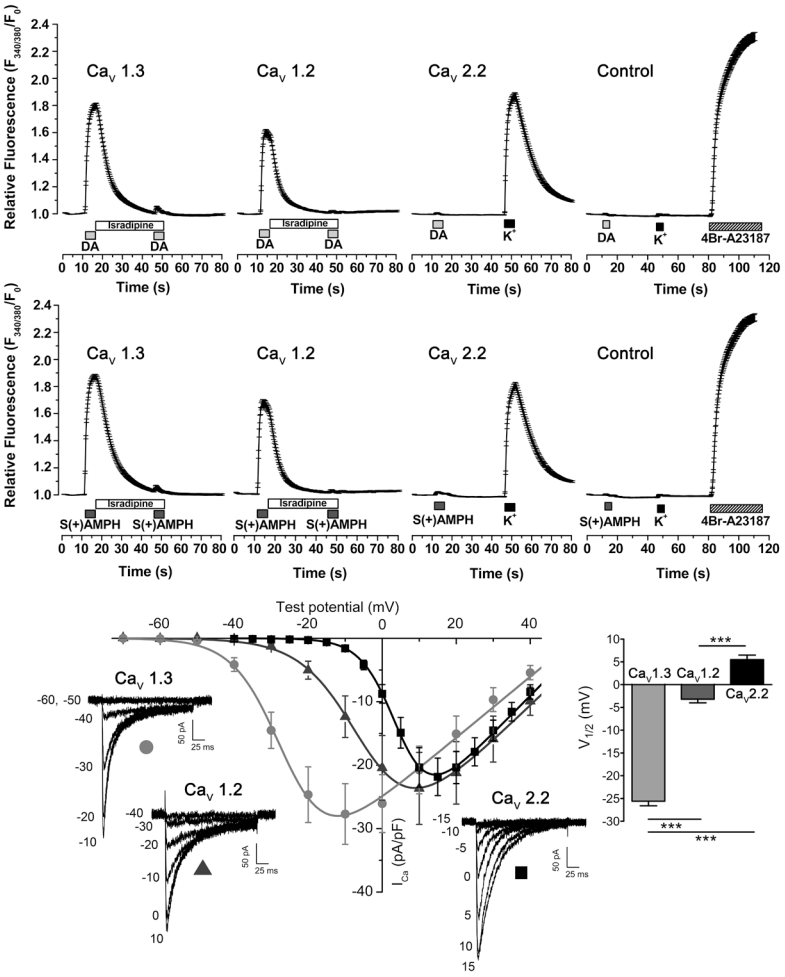

Figure 2. S(+)AMPH or DA activates Ca$_V$1.2 and Ca$_V$1.3, but not Ca$_V$2.2

(Upper and middle panel) Intracellular Ca^{2+} determinations in Fura-2AM loaded Flp-hDAT cells evaluated by fluorescence microcopy, under constant perfusion and at 35°C. Flp-hDAT cells were co-transfected with Ca$_V$1.3, Ca$_V$1.2 or Ca$_V$2.2 plus β_3, $\alpha_2\delta$ and EGFP plasmids. The α1 subunit was omitted from the plasmid transfection mix for the control condition. Transfected cells were identified by their EGFP signal and then briefly exposed to dopamine 10 μM (DA), S(+)AMPH 5 μM, high potassium external solution 130 mM (K^+, equimolar substitution of Na^+) or 4Br-A23187 (calcium ionophore, 5 μM) as indicated in the timeline of each panel. Isradipine (2 μM) averts Ca^{2+} signals induced by both hDAT substrates. Each trace constitutes the mean ± s.e.m. of n ≥ 81 cells per condition. (Lower panel) Voltage dependence of Ca$_V$1.2, Ca$_V$1.3 and Ca$_V$2.2- mediated Ca^{2+} currents: HEK293T cells were co-transfected with β3, α2δ, and EGFP expression plasmids plus alternatively Ca$_V$1.3, Ca$_V$1.2 or Ca$_V$2.2 plasmids. The Ca^{2+} current (I_{Ca}) recordings were carried out at room temperature under constant perfusion. Test pulses in 5 mV steps for Ca$_V$2.2 or 10 mV steps for Ca$_V$1.2 and Ca$_V$1.3 were applied from a holding potential of −80 mV. Representative responses are shown for Ca$_V$1.3 (light grey circle), Ca$_V$1.2 (dark grey triangle) and Ca$_V$2.2 (black square) and the magnitude of the test potentials are indicated in mV. The peak current density for the voltage steps were fit to Eq. 2 and yielded the following parameters: G_{max} =

497 ± 86, 560 ± 128 and 631 ± 77 (pS/pF); $V_{1/2}$ = −25.6 ± 1.0, −3.2 ± 0.8 and 5.5 ± 1.0 mV (***p < 0.001, one-way ANOVA, indicated in the figure); *k* = 6.7 ± 0.2, 7.7 ± 0.2 and 4.7 ± 0.1 (mV) for $Ca_V1.3$ (n = 8), $Ca_V1.2$ (n = 7) and $Ca_V2.2$ (n = 8), respectively.

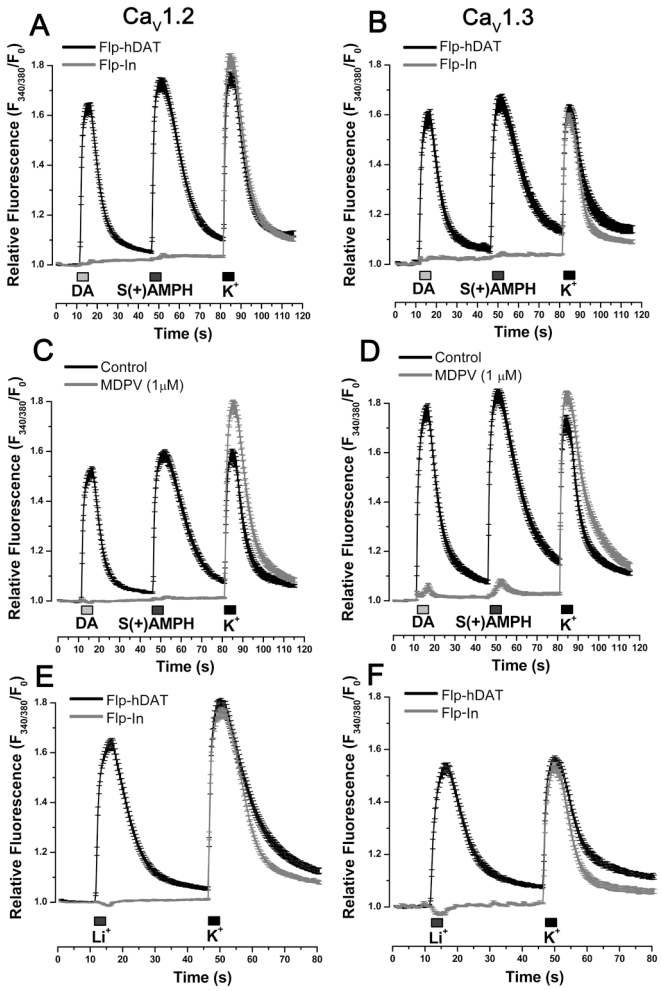

Figure 3. hDAT-mediated depolarization activates L-type Ca^{2+} channels in Flp-hDAT cells

Intracellular Ca^{2+} concentration was determined by fluorescence microscopy in Flp-hDAT or the parental Flp-In™ T-REx™ 293 (Flp-In) cells (no hDAT expression) cells co-transfected with $Ca_V1.2$ (A, C, E) or $Ca_V1.3$ (B, D,F) plus β_3, $\alpha_2\delta$ and EGFP plasmids, using the Ca^{2+} sensitive dye Fura-2AM. The experiments were carried out under constant perfusion at 35°C. The transfected cells were identified by their EGFP signal. A, B. Cells were briefly exposed to DA 10 μM, S(+)AMPH 5 μM or high potassium external solution 130 mM (K^+) as indicated in each panel. C, D. The blockade of hDAT with methylenedioxypyrovalerone (MDPV, 1 μM) prevented Ca^{2+} signals induced by hDAT substrates. E, F. Cells were exposed to external solution containing Li^+ (equimolar substitution of Na^+) or external solution with high potassium as indicated in the timeline of each panel. Li^+-induced Ca^{2+} signals only take place in cells expressing hDAT. Traces represent the mean ± s.e.m. of $n \geq 30$ cells per condition.

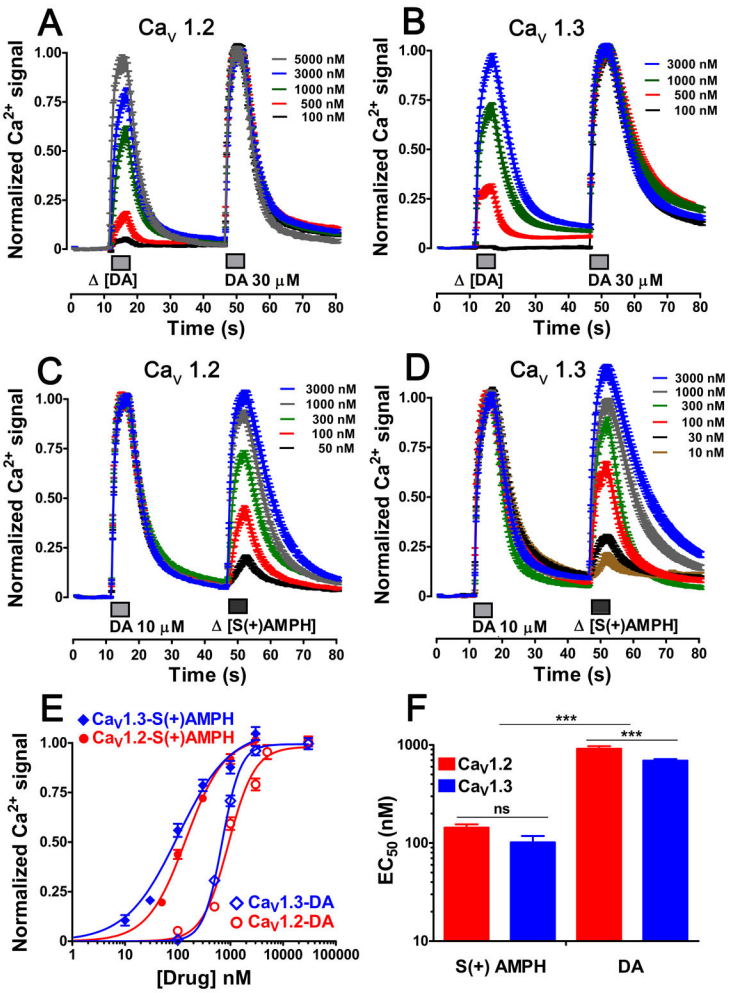

Figure 4. S(+)AMPH is more potent than DA producing Ca^{2+} signals in L-type Ca^{2+} channel-expressing Flp-hDAT cells

Intracellular Ca^{2+} signals were monitored using the calcium sensitive dye Fura-2AM and epifluorescence microscopy. Three days prior to each experiment Flp-hDAT cells were co-transfected with $Ca_V1.3$ or $Ca_V1.2$ plus β_3, $\alpha_2\delta$ and EGFP plasmids. The EGFP was used as transfection marker. (A, B, C, D) The potency of each compound was calculated using a two-pulse protocol, where one fixed saturating concentration pulse of dopamine works as an internal calibration and a variable concentration pulse was applied to get a dose-response curve. The traces represent the mean ± s.e.m. of n ≥ 48 cells per concentration. E. The dose-response curve was obtained fitting the responses to the Eq.1; cells expressing $Ca_V1.3$ the EC_{50} values and Hill slope were: 693 ± 25 and 102*** ±16 nM (***p < 0.001 one way ANOVA) and 2.5 ± 0.2 and 0.9*** ± 0.1 (***p < 0.001 one way ANOVA) for dopamine and S(+)amphetamine, respectively. Cells expressing $Ca_V1.2$ the EC_{50} values and Hill slope were: 916 ± 54 and 144*** ± 11 nM (***p < 0.001 one way ANOVA) and 1.7 ± 0.2 and 1.2 ± 0.1 for DA and S(+)AMPH, respectively, and (F) for better comparison the EC_{50} values are plotted.

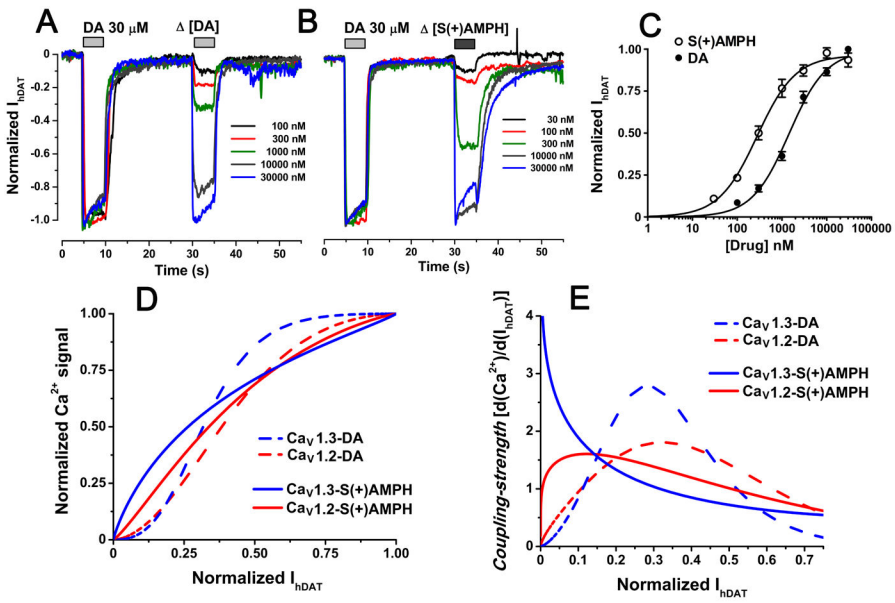

Figure 5. S(+)AMPH-induced currents are electrically favored to activate L-type Ca^{2+} channels

Ionic currents were determined by voltage-clamp in whole cell configuration under constant perfusion at 35°C. (A and B) Flp-hDAT cells clamped at −60 mV were exposed to a constant DA calibration pulse and a variable pulse of DA or S(+)AMPH; representative traces for the indicated concentrations tested are depicted in each panel. C. The full dose-response curves were fit to Eq.1 and yield the following parameters: EC_{50} = 1.44 ± 0.24 μM and 0.28** ± 0.04 μM (**p < 0.01, *t*-test) and Hill Slope = 1.1 ± 0.1 and 1.0 ± 0.1 for DA and S(+)AMPH, respectively. Each point indicates mean ± s.e.m. of n ≥ 5 current determinations for each concentration. D. The fitted S(+)amphetamine and dopamine Ca^{2+} signals on Fig. 4E were plotted as a function of the fitted hDAT currents and (E) the *coupling-strength* index was computed as the first derivative of the Ca^{2+} signal – hDAT current curves.